Adaptive Observers Applied to Pan Temperature Control of Induction Hobs

David Paesa, Sergio Llorente, Carlos Sagüés, and Óscar Aldana

***Abstract*—In this paper, a pan temperature control of induction hobs is described. The aim is that the user may select the cooking temperature instead of the power for the cooker. Pan temperature has to be estimated from a thermal sensor placed under the ceramic glass. Heat transmission from the induction coil to the pan and from the pan to the thermal sensor is modeled using a state-space model. As induction heating is highly dependent on thermal and magnetic pan properties, two different adaptive schemes are proposed and compared. Both guarantee a proper closed loop behavior. The contribution of this paper is related with temperature adaptive observer for different pans. The resultant system is simple, user friendly, robust, and safe, and is used for automatic cooking.**

***Index Terms*—Adaptive observer, home appliance, induction hobs, multiple models, temperature control.**

I. Introduction

IN DOMESTIC induction hobs [13], an inverter topology supplies a high-frequency current to an induction coil, producing an alternating magnetic field. If this field is applied to a ferromagnetic pan, it will produce eddy currents and magnetic hysteresis, which heat up the pan.

Controlling the pan temperature ensure a correct food cooking. Long overshoot might burn the food and long undershoot either increases cooking time, or causes underdone food. Therefore, accurate pan temperature control is very interesting.

Several solutions for this problem have been developed. A precursor work [1] used a temperature sensor that had to be put into the food to ensure a proper control. A later development was an infrared sensor [2] which measured the temperature on the side of the pan to control the food temperature [3]. This has two main inconveniences: The first one is that infrared sensor only works properly when the liquid used in the cooking process (either water or oil) has at least the same height than the infrared sensor. The second one is that the infrared sensors are complex from the electronic point of view, because they need a concave mirror to focus the radiation into an isolated membrane and a series connection of thermocouples to measure the temperature of the membrane, which represents the temperature of the emitting surface.

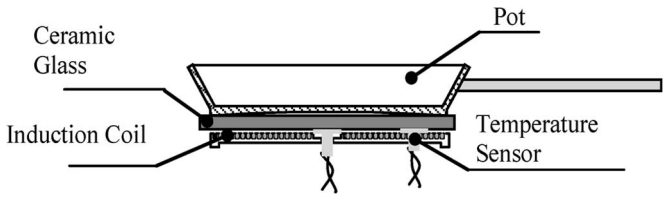

Fig. 1. Elements of an induction hob.

In this paper, we propose to use a temperature sensor placed over the coil, to measure the ceramic glass temperature, as is shown in Fig. 1. Therefore, we solve both disadvantages presented in [3]. Using a negative temperature coefficient (NTC) thermistor, we have a solution simpler than the previous ones. Besides, measuring below the pan, we are able to estimate the pan temperature even we are cooking with small amount of food.

Thermal process comes up as follows. Heat is produced on the pan surface directly, and it is transmitted to the induction coil going through the ceramic glass. That heat produced in the pan is highly dependent on the pan magnetic properties. Besides, the heat transmitted through the ceramic glass is dependent on the pan bottom evenness. Therefore, an adaptive observer, whose parameters can be adapted online, is required.

Two different adaptive schemes are compared: The first one is a conventional adaptive observer whose parameters are tuned to ensure a suitable behavior [4]–[6], whereas the second one uses a finite number of models from which one has to be chosen as the best approximation of the real plant [7], [8].

In this paper, a pan temperature control of induction hobs is presented. It works independent of both: the used pan and the amount of food. A state-space model is used to simulate the relation between the system temperatures and the power supplied by the coil. Power supplied can be calculated from the used inverter topology [9], [11], [12] and pan temperature is estimated, from the ceramic glass temperature measurement using either an adaptive observer [6], or an adaptive observer based on multiple models in a similar way that have been used for adaptive control [8].

Paper MSDAD-08-031, presented at the 2007 Seminar for Advanced Industrial Control Applications, Madrid, Spain, November 5–6, and approved for publication in the IEEE TRANSACTIONS ON INDUSTRY APPLICATIONS by the Industrial Automation and Control Committee of the IEEE Industry Applications Society. Manuscript submitted for review January 30, 2008 and released for publication November 20, 2008. Current version published May 20, 2009. This work was supported in part by the BSH Home Appliances Group.

D. Paesa and Ó. Aldana are with the Research and Development Department, Induction Technology, Product Division Cookers, BSH Home Appliances Group, 50016 Zaragoza, Spain (e-mail: david.paesa-ext@bshg.com).

S. Llorente is with the Research and Development Department, Induction Technology, Product Division Cookers, BSH Home Appliances Group, 50016 Zaragoza, Spain, and also with the University of Zaragoza, 50018 Zaragoza, Spain (e-mail: sergio.llorente@bshg.com).

C. Sagüés is with the Department of Computer Science and Systems Engineering—Aragon Institute of Engineering Research, University of Zaragoza, 50018 Zaragoza, Spain (e-mail: csagues@unizar.es).

Color versions of one or more of the figures in this paper are available online at http://ieeexplore.ieee.org.

Digital Object Identifier 10.1109/TIA.2009.2020189

0093-9994/$25.00 © 2009 IEEE

Authorized licensed use limited to: Universidad de Zaragoza. Downloaded on May 21, 2009 at 10:45 from IEEE Xplore. Restrictions apply.

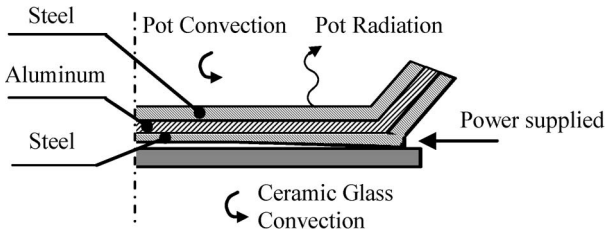

Fig. 2. Thermal scheme, representing pan layers and different heat losses.

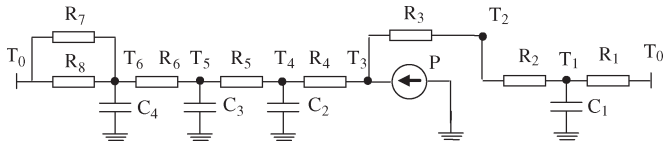

Fig. 3. Equivalent thermal circuit of the system.

This paper is organized as follows. First, the thermal behavior of the system is described. The equivalent thermal circuit obtained is used to develop a space state model of the induction hob system. Afterward, two different methods to estimate the pan temperature are described. Finally, real tests for different pans and control schemes are presented. A conventional PID controller without an adaptive observer and two different adaptive estimation strategies are compared in order to underline the obligation of use adaptive observers.

II. State-Space Model of the Induction System

A complete study, not only of the heat transmission but also of the pan construction, is needed to make an accurate system model. Most pans are made of on aluminum layer between two thin steel layers; therefore, this pan construction is assumed on our model.

Furthermore, all heat losses have to be considered. There are several heat losses in our system: a radiation loss from the pan to the air, a convection loss from the pan to the air, and a convection loss from the ceramic glass to the air. Thermal scheme is shown in Fig. 2.

This system can be regarded as an electric circuit, where electrical voltages represent temperatures, electrical current represent heat transmission, electrical capacitors represent thermal capacities, and every heat flow is represented by a resistor. The equivalent thermal circuit of the system is shown in Fig. 3. Table I summarizes the meaning of each element used in Fig. 3.

Heat transmission is produced as follows. First, the heat is produced directly on the pan bottom, and it is transmitted up, through the pan layers, and down, through the ceramic glass. Besides, both pan and ceramic glass have losses. The pan has losses to the air, through radiant and convection resistors, and the ceramic glass has losses to the air, by means of convection resistor. There is also, a contact resistor between pan and ceramic glass which represents the pan bottom evenness.

Once an equivalent thermal circuit of the system is obtained, and assuming that we know the values of each resistor and capacitor, we are able to calculate the temperature of each node by means of Kirchoff laws, using

TABLE I
Elements Used in Fig. 3

T_O	Temperature of the air.
T_1	Temperature below the ceramic glass.
T_2	Temperature over the ceramic glass.
T_3	Temperature of the lower steel layer.
T_4	Temperature of the aluminium layer.
T_5	Temperature of the upper steel layer.
T_6	Temperature of the upper pot surface.
R_1	Convection resistor from ceramic glass to air.
R_2	Conduction resistor of the ceramic glass.
R_3	Contact resistor between ceramic glass and pot.
R_4	Conduction resistor of the lower steel layer.
R_5	Conduction resistor of the aluminum layer.
R_6	Conduction resistor of the upper steel layer.
R_7	Convection resistor from pot to air.
R_8	Radiation resistor from pot to air.
C_1	Ceramic glass heat capacity.
C_2	Lower steel layer heat capacity.
C_3	Aluminum layer heat capacity.
C_4	Upper steel layer heat capacity.
P	Power supplied by the induction coil.

$$\frac{T_2(t)-T_1(t)}{R_2}=\frac{T_1(t)-T_0}{R_1}+\frac{C_1\cdot\partial T_1(t)}{\partial t} \tag{1}$$

$$\frac{T_3(t)-T_2(t)}{R_3}=\frac{T_2(t)-T_1(t)}{R_2} \tag{2}$$

$$P(t)=\frac{T_3(t)-T_2(t)}{R_3}+\frac{T_3(t)-T_4(t)}{R_4} \tag{3}$$

$$\frac{T_3(t)-T_4(t)}{R_4}=\frac{T_4(t)-T_5(t)}{R_5}+\frac{C_2\cdot\partial T_4(t)}{\partial t} \tag{4}$$

$$\frac{T_4(t)-T_5(t)}{R_5}=\frac{T_5(t)-T_6(t)}{R_6}+\frac{C_3\cdot\partial T_5(t)}{\partial t} \tag{5}$$

$$\frac{T_5(t)-T_6(t)}{R_6}=\frac{T_6(t)-T_0}{R_7}+\frac{T_6(t)-T_0}{R_8}+\frac{C_4\cdot\partial T_6(t)}{\partial t}. \tag{6}$$

Therefore, the relation between the power supplied by the induction coil and the temperatures can be calculated and represented by a state-space model using

$$\begin{aligned} x(t)&=A\cdot x(t)+B\cdot u(t), \qquad x\in R^n;\quad u\in R^m\\ y(t)&=C\cdot x(t)+D\cdot u(t), \qquad y\in R \end{aligned} \tag{7}$$

Authorized licensed use limited to: Universidad de Zaragoza. Downloaded on May 21, 2009 at 10:45 from IEEE Xplore. Restrictions apply.

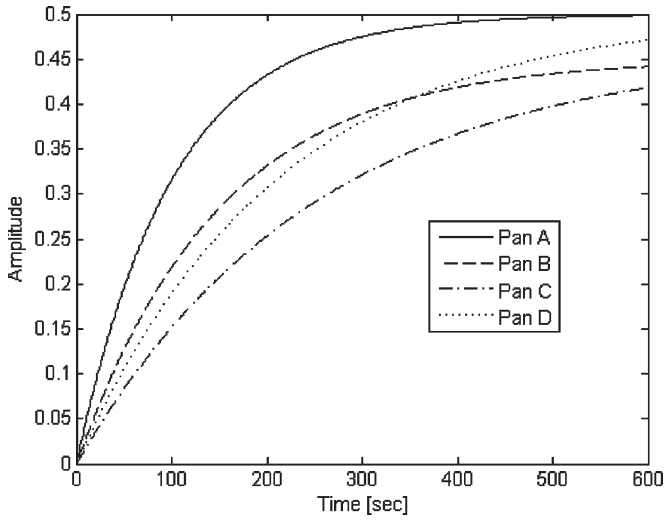

Fig. 4. (A) Represents the reference model step response. (B–D) Represent the step responses of other different pans.

where $x(t)$ is the state vector which includes the temperatures of the system, $u(t)$ is the input vector, $y(t)$ is the output vector, A is state matrix, and B is the input matrix.

Note that the values of the resistors and capacitors are highly dependent on the pan thermal properties. Therefore, there will be one different state-space model for each pan. The modeling process was repeated for all the available pans; hence, a database with more than 150 simulation models was obtained.

From all the obtained state-space models, the reference model is chosen as the model which reaches the highest pan temperature for the same supplied power. Step response for the most characteristic pans is shown in Fig. 4. In this case, the solid line would represent the course of the reference model because its step response is the highest.

The definition of a reference model in this way will be rather useful to avoid pan temperature overshooting until the estimation of the pan temperature finishes.

III. Control Schemes

During the cooking process, it is not possible to know which pan is being used. Consequently, an online scheme to determine the state-space model for each pan is needed.

Two different ways to solve that problem are proposed and compared. The first one uses an adaptive observer which needs auxiliary signals in order to ensure a good estimation of the system parameters, while the second one solves the problem using an adaptive observer based on multiple models.

Both control schemes have to achieve three goals. First, they have to ensure that any pan reaches the target temperature with an overshoot less than 10%. Second, they have to hold the pan temperature in the set point with a steady state offset less than 5%. Finally, they have to bring the pan temperature to the target temperature as fast as possible.

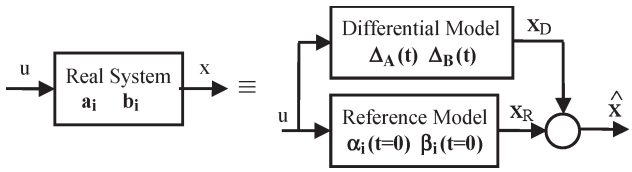

Fig. 5. Equivalent model of a real system.

A. Adaptive Observer

In this case, it is assumed that each real pan can be modeled as the combination of a reference model and a differential model. The differential model represents the different thermal and magnetic properties between the real model and the reference model. This scheme is shown in Fig. 5.

As it is shown above, reference model reaches higher pan temperatures for the same power supplied. Therefore, adaptive observer starts using the reference model parameters to estimate the pan temperature until real the pan parameters are obtained. If a pan with different properties than the reference model is used, then a pan temperature estimation greater than real temperature will be guaranteed. Consequently, real pan temperature overshoot is avoided

$$\begin{aligned} \dot{x}(t) &= A \cdot x(t) + B \cdot u(t) + B \cdot d(t) \\ y(t) &= C \cdot x(t) + D \cdot u(t) \end{aligned} \tag{8}$$

where $x(t)$ is the state vector, $u(t)$ is the control vector, $y(t)$ is the system output vector, and $d(t)$ is the disturbance vector. It is shown in [6] that only if the system described in (8) is completely observable, then it can be represented in the following form:

$$\begin{bmatrix} \dot{x}_1 \\ \dot{x}_2 \\ \cdot \\ \cdot \\ \dot{x}_n \end{bmatrix} = \begin{bmatrix} a_1 & 1 & 1 & \cdot & 1 \\ a_2 & -\lambda_2 & 0 & \cdot & 0 \\ \cdot & 0 & \cdot & \cdot & \cdot \\ \cdot & \cdot & \cdot & \cdot & 0 \\ a_n & 0 & \cdot & 0 & -\lambda_n \end{bmatrix} \cdot \begin{bmatrix} x_1 \\ x_2 \\ \cdot \\ \cdot \\ x_n \end{bmatrix} + \begin{bmatrix} b_1 \\ b_2 \\ \cdot \\ \cdot \\ b_n \end{bmatrix} \cdot u + \begin{bmatrix} d_1 \\ 0 \\ \cdot \\ \cdot \\ 0 \end{bmatrix} \cdot u$$
$$y = (1 \quad 0 \quad \cdots \quad 0)x = x_1 \tag{9}$$

where $\lambda_i (i = 2, \ldots, n)$ are arbitrary and known constant, $a = (a_1 \quad a_2 \quad \cdots \quad a_n)^{\mathrm{T}}$ and $b = (b_1 \quad b_2 \quad \cdots \quad b_n)^{\mathrm{T}}$ are the system parameters which have to be estimated and $d = (d_1 \quad 0 \quad \cdots \quad 0)^{\mathrm{T}}$ are the disturbance parameters which are applied to the system.

Therefore, the adaptive observer will have a form similar to (9) but whose parameters $\alpha = (\alpha_1 \quad \alpha_2 \quad \cdots \quad \alpha_n)^{\mathrm{T}}$, $\beta = (\beta_1 \quad \beta_2 \quad \cdots \quad \beta_n)^{\mathrm{T}}$ and $\partial = (\partial_1 \quad 0 \quad \cdots \quad 0)^{\mathrm{T}}$ will be

Authorized licensed use limited to: Universidad de Zaragoza. Downloaded on May 21, 2009 at 10:45 from IEEE Xplore. Restrictions apply.

adjusted adaptively in order to match those of the system (9) as $t \to \infty$

$$\begin{bmatrix} \dot{\hat{x}}_1 \\ \dot{\hat{x}}_2 \\ \cdot \\ \cdot \\ \dot{\hat{x}}_n \end{bmatrix} = \begin{bmatrix} \alpha_1 & 1 & 1 & \cdot & 1 \\ \alpha_2 & -\lambda_2 & 0 & \cdot & 0 \\ \cdot & 0 & \cdot & \cdot & \cdot \\ \cdot & \cdot & \cdot & \cdot & 0 \\ \alpha_n & 0 & \cdot & 0 & -\lambda_n \end{bmatrix} \cdot \begin{bmatrix} x_1 \\ \hat{x}_2 \\ \cdot \\ \cdot \\ \hat{x}_n \end{bmatrix} + \begin{bmatrix} \beta_1 \\ \beta_2 \\ \cdot \\ \cdot \\ \beta_n \end{bmatrix} \cdot u + \begin{bmatrix} \partial_1 \\ 0 \\ \cdot \\ \cdot \\ 0 \end{bmatrix} \cdot u + \begin{bmatrix} -\lambda_1(\hat{x}_1 - x_1) \\ \omega_2 \\ \cdot \\ \cdot \\ \omega_n \end{bmatrix}$$

$$\partial_1 = L_I(\hat{x}_1 - x_1) \tag{10}$$

where L_I is a gain which can be calculated by means of any eigenvalue assignment method and $\omega = (\omega_2 \quad \cdots \quad \omega_n)^{\mathrm{T}}$ are the auxiliary signals that are calculated as follows:

$$\omega_i = -\left(c_i \cdot v_i^2 + d_i \cdot s_i^2\right) \cdot (\hat{x}_i - x_i), \qquad i = 2, \ldots, n. \tag{11}$$

Subtracting (9) from (10), we obtain the equation of the estimation error $e_i = \hat{x}_i - x_i$

$$\begin{bmatrix} \dot{e}_1 \\ \dot{e}_2 \\ \cdot \\ \cdot \\ \dot{e}_n \end{bmatrix} = \begin{bmatrix} -\lambda_1 & 1 & 1 & \cdot & 1 \\ 0 & -\lambda_2 & 0 & \cdot & 0 \\ \cdot & 0 & \cdot & \cdot & \cdot \\ \cdot & \cdot & \cdot & \cdot & 0 \\ 0 & 0 & \cdot & 0 & -\lambda_n \end{bmatrix} \cdot \begin{bmatrix} e_1 \\ e_2 \\ \cdot \\ \cdot \\ e_n \end{bmatrix} + \begin{bmatrix} \phi_1 \\ \phi_2 \\ \cdot \\ \cdot \\ \phi_n \end{bmatrix} \cdot x_1 + \begin{bmatrix} \psi_1 \\ \psi_2 \\ \cdot \\ \cdot \\ \psi_n \end{bmatrix} \cdot u + \begin{bmatrix} \varphi_1 \\ 0 \\ \cdot \\ \cdot \\ 0 \end{bmatrix} \cdot u + \begin{bmatrix} 0 \\ \omega_2 \\ \cdot \\ \cdot \\ \omega_n \end{bmatrix} \tag{12}$$

where $\phi_i = \alpha_i - a_i$, $\psi_i = \beta_i - b_i$ $(i = 1, \ldots, n)$ and $\varphi_1 = \partial_1 - d_1$ are the parameter errors between the system (9) and the model (10).

Note that the parameters of the differential model can be calculated at every instant as

$$\begin{aligned} \Delta_A(t) &= \alpha_i(t) - \alpha_i(t=0) \\ \Delta_B(t) &= \beta_i(t) - \beta_i(t=0). \end{aligned} \tag{13}$$

Adaptive process can be summarized in the next four steps.

1) Generate auxiliary signals

$$\begin{aligned} \dot{v}_i + \lambda v_i &= x_1, \qquad i = 2, \ldots, n \\ \dot{s}_i + \lambda s_i &= u, \qquad i = 2, \ldots, n. \end{aligned} \tag{14}$$

2) Update parameter equations

$$\begin{aligned} \dot{\alpha}_1 &= -c_1 \cdot x_1(\hat{x}_1 - x_1) \quad \dot{\beta}_1 = -d_1 \cdot u(\hat{x}_1 - x_1) \\ \dot{\alpha}_2 &= -c_2 \cdot v_2(\hat{x}_1 - x_1) \quad \dot{\beta}_2 = -d_2 \cdot s_2(\hat{x}_1 - x_1) \\ &\cdot \qquad\qquad\qquad\quad \cdot \\ &\cdot \qquad\qquad\qquad\quad \cdot \\ \dot{\alpha}_n &= -c_n \cdot v_n(\hat{x}_1 - x_1) \quad \dot{\beta}_2 = -d_n \cdot s_n(\hat{x}_1 - x_1) \end{aligned} \tag{15}$$

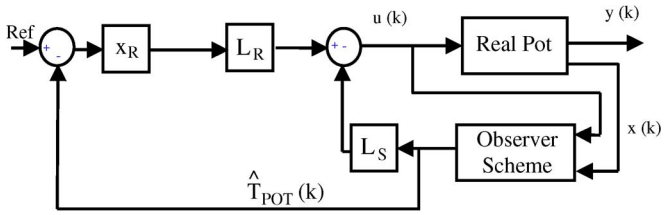

Fig. 6. Block diagram of the control scheme.

where c_i and d_i $(i = 1, \ldots, n)$ are arbitrary but positive gains.

3) Update disturbance equations

$$\partial_1 = L_I(\hat{x}_1 - x_1). \tag{16}$$

4) Update model equations

$$\begin{aligned} \dot{x}_1 &= \alpha_1 \cdot x_1 + \hat{x}_2 + \cdots + \hat{x}_n + \beta_1 \cdot u + \partial_1 \cdot u - \lambda_1 \cdot (\hat{x}_1 - x_1) \\ \dot{\hat{x}}_2 &= \alpha_2 \cdot x_1 - \lambda_2 \cdot \hat{x}_2 + \beta_2 \cdot u + \left(c_2 v_2^2 + d_2 s_2^2\right) \cdot (\hat{x}_1 - x_1) \\ &\cdot \qquad\qquad\qquad\qquad \cdot \\ \dot{\hat{x}}_n &= \alpha_n \cdot x_1 - \lambda_n \cdot \hat{x}_n + \beta_n \cdot u + \left(c_n v_n^2 + d_n s_n^2\right) \cdot (\hat{x}_1 - x_1). \end{aligned} \tag{17}$$

A further insight in adaptive observers with auxiliary signals is explained in [6], where both stability and converge of this scheme is proved.

In order to accomplish the control requirements, a state-space controller with integrators is used. Note that power supplied by the induction coil is constrained by the inductor diameter; therefore, an antiwindup scheme was needed to compensate this saturation. As is shown in Fig. 6, control law employs two different gains to ensure a proper performance. Action provided by the controller can be calculated as follows:

$$u(t) = -L_{\mathrm{S}} \cdot x_{\mathrm{S}} + L_{\mathrm{R}} \cdot x_{\mathrm{R}} \tag{18}$$

where L_{S} represents the state-space variables gain, L_{R} represents the integration gain, x_{S} represents the state-space variables, and x_{R} represents the integrated reference error. These gains can be easily calculated using a pole placement method.

Control scheme starts using a control law calculated to guarantee a proper control for the reference model. Unfortunately, this control law has a poor performance with pans of different thermal property.

Initial control law is calculated in order to minimize overshooting for different pans to the reference model. Therefore, it is guaranteed that any pan does not reach dangerous temperatures while the adaptive observer is estimating the pan parameters.

Once the adaptive observer solution converges, the parameters obtained $\alpha = (\alpha_1 \quad \alpha_2 \quad \cdots \quad \alpha_n)^{\mathrm{T}}$ and $\beta = (\beta_1 \quad \beta_2 \quad \cdots \quad \beta_n)^{\mathrm{T}}$ are used to update the control law. Controller switches its control law in function of the parameters estimated by the adaptive observer.

In simulation, these new gains can be easily calculated online; however, that computation is rather complex

Authorized licensed use limited to: Universidad de Zaragoza. Downloaded on May 21, 2009 at 10:45 from IEEE Xplore. Restrictions apply.

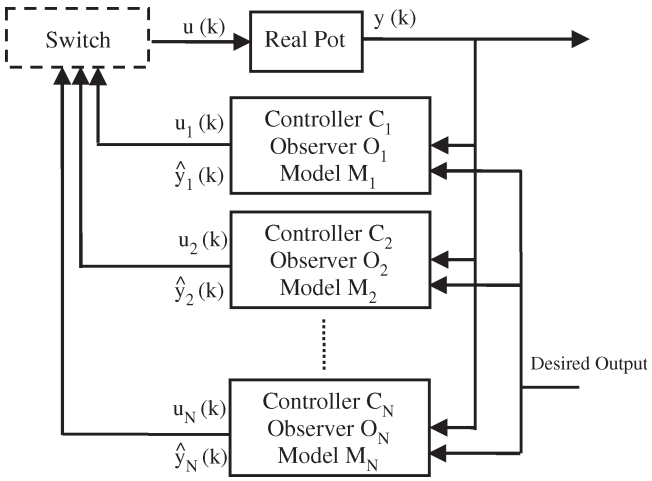

Fig. 7. Adaptive control using multiple model.

to do with a microcontroller. Therefore, L_{S} and L_{R} gains for different values of $\alpha = (\alpha_1 \quad \alpha_2 \quad \cdots \quad \alpha_n)^{\mathrm{T}}$ and $\beta = (\beta_1 \quad \beta_2 \quad \cdots \quad \beta_n)^{\mathrm{T}}$ are calculated offline and programmed in the microcontroller as a lookup table.

B. Multiple Model Observer

Conventional robust control reacts too slowly to large changes in the plant parameters, and therefore large errors between estimation and real pot temperature occur before the solution converges.

That transient behavior can be improved using multiple models. The idea of multiple models has been previously used for control [8]. Our problem is more related to obtain good estimations, and we have multiple models to estimate the pot temperature from the temperature measured through the NTC. The information of all the pots previously identified is used to develop multiple models representing most of the possible pots. A controller and an observer for each identified model, which manage all control requirements shown above, are also calculated and tuned. Therefore, the control strategy proposed is to determine the best model for the current real pot at every instant just to use the corresponding observer and controller.

Flowchart of that scheme is shown in Fig. 7. The main objective is to make the control error tend to zero. The control scheme has N models denoted by $\{M_j\}_{j=1}^{N}$, and each one has associated one controller C_j and one observer O_j.

Each one of these observers calculates a estimated output $\hat{y}_j(t)$ which is used to calculate the estimation error every sample time, denoted by $e_j(k) = \hat{y}_i(k) - y(k)$. At every instant, one of the models M_j is chosen by a switching rule based on a performance cost index. Afterward, the corresponding observer calculates the control error as

$$e_C(k) = r(k) - \hat{y}_i(k) \tag{19}$$

where $r(k)$ is the desired output and $\hat{y}_i(t)$ is the estimation of the observer associated to the model selected. Finally, the corresponding controller C_j calculates its control input u_j depending on the $e_C(k)$ which is given to the plant.

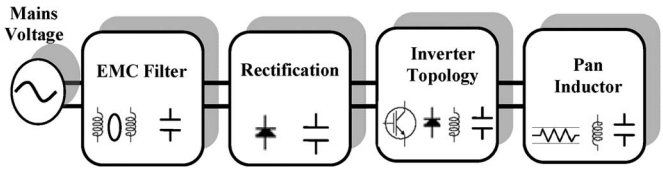

Fig. 8. Arrangement of the induction hob.

Fig. 9. Induction hob board with a half-bridge inverter topology.

Different performance cost indexes have been proposed to determine the best model and its corresponding controller. All of them are based on the performance of the models rather than of the controllers, i.e., using $e_j(t)$ instead of $e_C(t)$.

Therefore, the performance index used has the following form [8]:

$$J_j(t) = \alpha e_j^2(t) + \beta \int_0^k e^{-\lambda(k-\tau)} e_j^2(\tau) d\tau, \qquad \alpha \geq 0; \beta, \lambda > 0 \tag{20}$$

where α and β are chosen as weighting factors of the current and integrated estimation errors. λ is the forgetting factor, which determines the memory of the cost index. In our case, $\lambda = 0$ is used meaning that performance cost index is calculated every instant.

Note that a finite number of models are used to represent an infinite number of possible real pots. Therefore, to find a perfect match between the selected model and the real pot is not usual. Adaptation or tuning of one or more models may be needed to increase the control performance.

IV. Implementation

Simulation algorithms have been programmed using Matlab whereas real-time algorithms for hob microcontroller have been programmed in C language. The following control schemes have been tested and compared. First, a conventional PID controller without an adaptive observer has been analyzed in order to highlight the benefits of using an adaptive observer strategy. Afterward, previous observer strategies are tested: including not only the adaptive observer but also the multimodel observer.

In order to verify that each control schemes work properly, several verification tests on real induction hob were done. An

Authorized licensed use limited to: Universidad de Zaragoza. Downloaded on May 21, 2009 at 10:45 from IEEE Xplore. Restrictions apply.

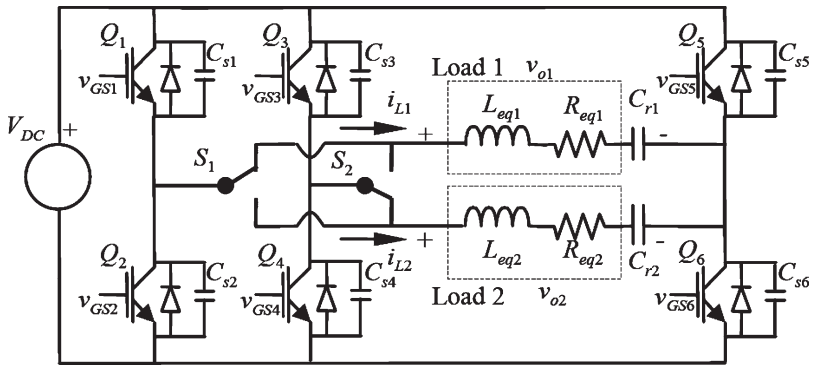

Fig. 10. Two-output full-bridge resonant inverter implementation.

induction hob was selected due to its specific features of safety, cleanliness, quick warming, and high efficiency. Induction hobs have an efficiency of 86% whereas conventional radiation hobs have an efficiency of 72%. The hob efficiency is determined measuring the energy needed to heat up 2 L of water from 15 °C to 90 °C. The proposed control schemes do not modify the efficiency of the hob, because the energy needed to heat up the water is the same.

Arrangement of the induction hob used is shown in Figs. 8 and 9. Hob takes the energy from the mains voltage; afterward, an electromagnetic compatibility filter removes the voltage disturbances, which is subsequently rectified by a full bridge of diodes. Finally, the inverter topology provides to the induction coil the high-frequency current needed to heat up the pan. This can be seen as a resonant load [9], [13].

The inverter topology used is the full-bridge two-output inverter [10] (Fig. 10). It is based on a shared common leg, and it is also based on adding two low-cost relays (S1, S2) to make parallel the independent legs when only one output is required. Thus, the converter can be configured to supply either both outputs or only one. In addition, the circuit includes some resonant capacitors Cr1, Cr2, and some snubber capacitors Cs1–Cs6, in order to get a zero-voltage switching operation of main switches.

The power supplied can be controlled modifying the operating frequency of the inverter. It provides its nominal power when it is working at the resonant frequency of the resonant load. However, above the resonant frequency, the higher the frequency is, the lesser power is provided.

Besides, the power in the load may vary, for the same power reference, due to two reasons. First, the variations in mains voltage are transmitted as variations in power. Variations up to 7% are usually considered. Second, pots may have quite different electrical characteristics. Therefore, the equivalent resonant load circuit (usually a series RL circuit) has significant variations. Therefore, an accurate real-time power measurement is required in order to ensure that the power calculated by the controller is provided to the pan.

Different methods to power measuring in two-output resonant inverters have been proposed and compared [11]. In this case, power is calculated from the measurements of the current and the voltage, which are sensed in each inductor using a first-order sigma-delta [12].

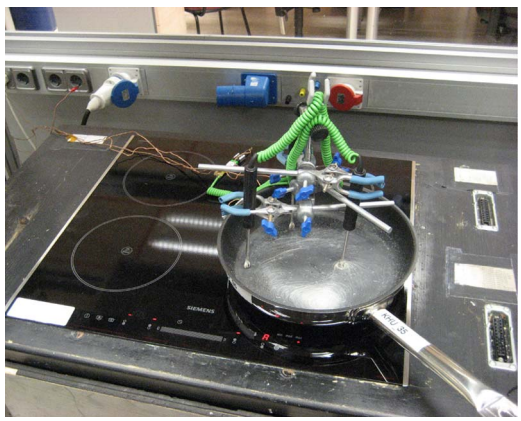

Fig. 11. Induction hob used in real experiments. Pan temperature is measured by three thermopiles.

During the verification tests, the system temperature evolution is measured for a set point of 200 °C. Additionally, a large disturbance has been forced adding water to the pot. Therefore, we can check the performance of each control scheme not only in usual situation but also in the presence of large disturbances. As it is shown in Fig. 11, the pan temperature was measured using thermopiles placed on the pan surface. Pan temperature is estimated by the algorithm in the microcontroller of the induction hob from the NTC thermistor measurements. Note that the algorithms do not need the temperatures measured by the three thermopiles. We use the three thermopiles placed on the pan surface only in the laboratory to measure its temperature just to register its evolution and to detect when the real pan temperature reaches the settling point. Therefore, the three thermopiles are not required in household conditions. As the NTC thermistor is placed below the ceramic glass the overall system is very user friendly.

The course of the power supplied by the induction coil, the temperature of the pan estimated, the temperature of the pan measured, and the temperature of the NTC thermistor for the different control schemes with different pots are shown in the following figures.

A. Conventional PID Controller Without Adaptive Observer

A conventional PID was designed to ensure a good performance for a pan with the same parameters than the reference

Authorized licensed use limited to: Universidad de Zaragoza. Downloaded on May 21, 2009 at 10:45 from IEEE Xplore. Restrictions apply.

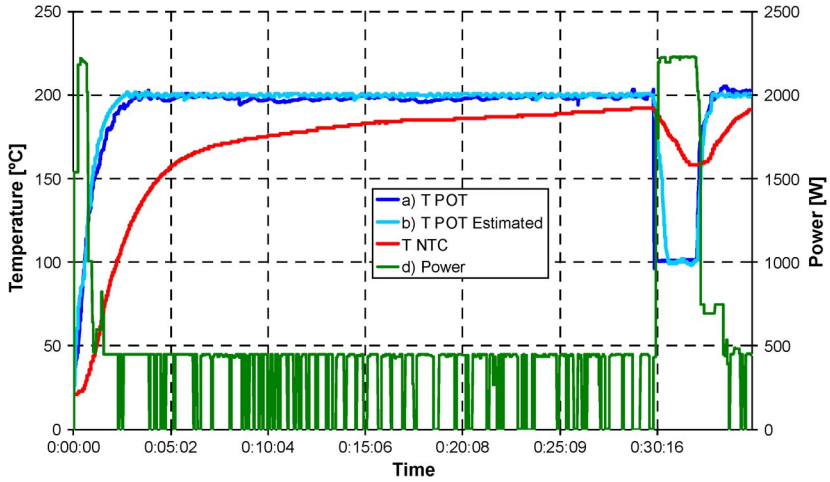

Fig. 12. Temporal course of a real test. Pan used is the reference model. (a) Represents the real pan temperature. (b) Represents the estimated pan temperature. (c) Represents the temperature measured by the NTC thermistor. (d) Represents the power supplied by the inductor.

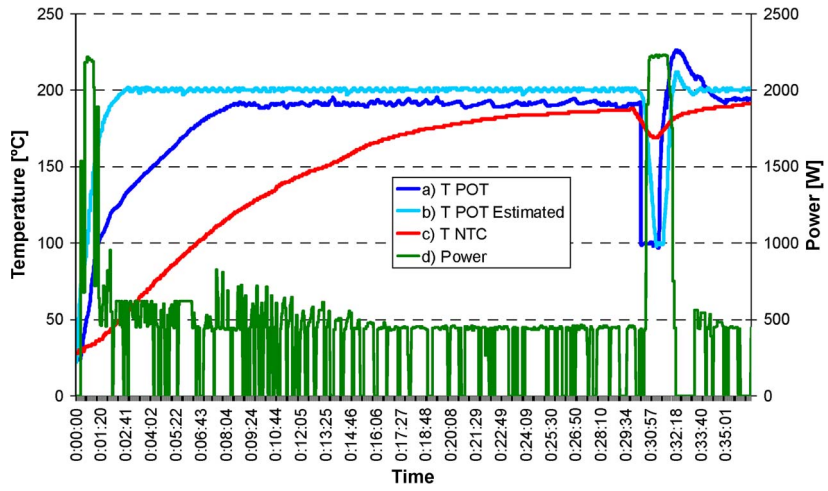

Fig. 13. Temporal course of a real test. Pan used has different thermal properties than the reference model. (a) Represents the real pan temperature. (b) Represents the estimated pan temperature. (c) Represents the temperature measured by the NTC thermistor. (d) Represents the power supplied by the inductor.

model. As the temperature of the pan is not accessible, an additional observer with the parameters of the reference model was also designed. Note that the parameters of that observer remain constant independently of the pot used.

Fig. 12 shows the performance of the PID controller without an adaptive observer testing a pot with the same parameters than the reference model. In this case, the estimated pot temperature and the real pot temperature are identical and the PID controller brings the pan temperature to the set point with an overshoot less than 4 °C and with ±3 °C of steady state offset. Besides, pan temperature reaches to reference in 2 min. In Fig. 13, the performance of the PID controller without an adaptive observer for a pot with different parameters than the reference model is shown. In this case, the estimated pot temperature and the real pot temperature are very different and the control performs badly.

B. Adaptive Observer

In Fig. 14, a real pan with the same thermal and magnetic properties than the reference model is used. Therefore, pan temperature measured and estimated are equal during the entire test. Controller brings the pan temperature to the set point with an overshoot less than 5 °C and with ±2 °C of steady state offset. Besides, pan temperature reaches reference in just 2 min.

In this case, control gains are not updated because solutions provided by the adaptive observer are equal to the parameters of the reference model.

In Fig. 15, a real pan with different thermal and magnetic properties than the reference model is tested. See how the pan temperature measured and the pan temperature estimated are different until adaptive observer solution converges (about 5 min). This overestimation, as it is shown above, is forced to ensure that pans with different properties to those of the reference model do not reach to dangerous temperatures.

When adaptive observer estimation finished, the control scheme updates the control laws depending on the parameters estimated by the adaptive observer using a lookup table.

Afterward, real and estimated pan temperature are equal ensuring a control without overshoot, not only when the system

Authorized licensed use limited to: Universidad de Zaragoza. Downloaded on May 21, 2009 at 10:45 from IEEE Xplore. Restrictions apply.

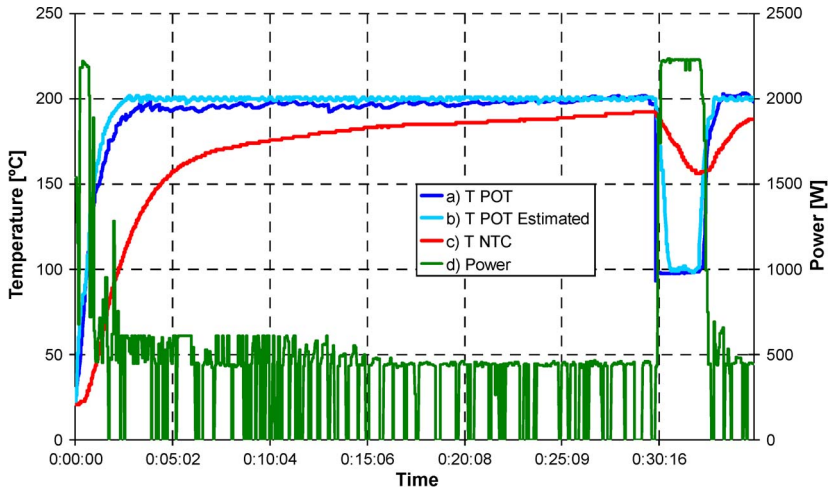

Fig. 14. Temporal course of a real test. Pan used is the reference model. (a) Represents the real pan temperature. (b) Represents the estimated pan temperature. (c) Represents the temperature measured by the NTC thermistor. (d) Represents the power supplied by the inductor.

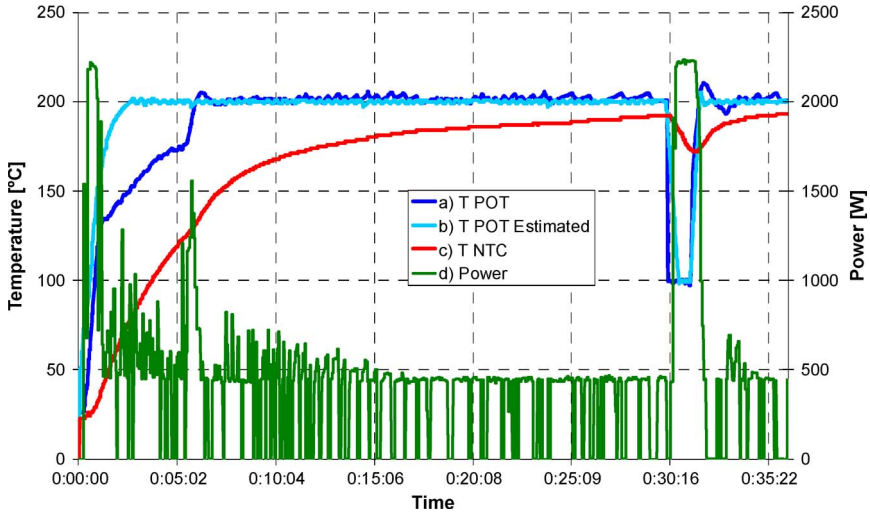

Fig. 15. Temporal course of a real test. Pan used has different thermal properties than the reference model. (a) Represents the real pan temperature. (b) Represents the estimated pan temperature. (c) Represents the temperature measured by the NTC thermistor. (d) Represents the power supplied by the inductor.

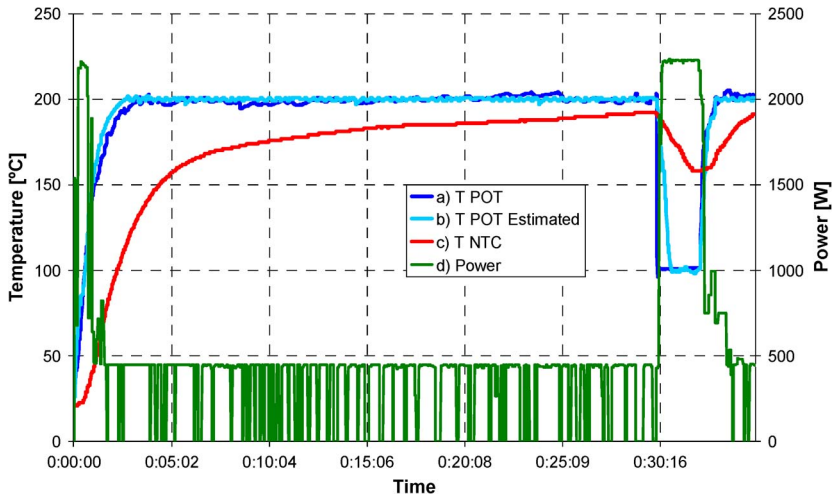

Fig. 16. Temporal course of a real test. Pan used is the reference model and the model chosen has the same thermal properties than the reference model. (a) Represents the real pan temperature. (b) Represents the estimated pan temperature. (c) Represents the temperature measured by the NTC thermistor. (d) Represents the power supplied by the inductor.

Authorized licensed use limited to: Universidad de Zaragoza. Downloaded on May 21, 2009 at 10:45 from IEEE Xplore. Restrictions apply.

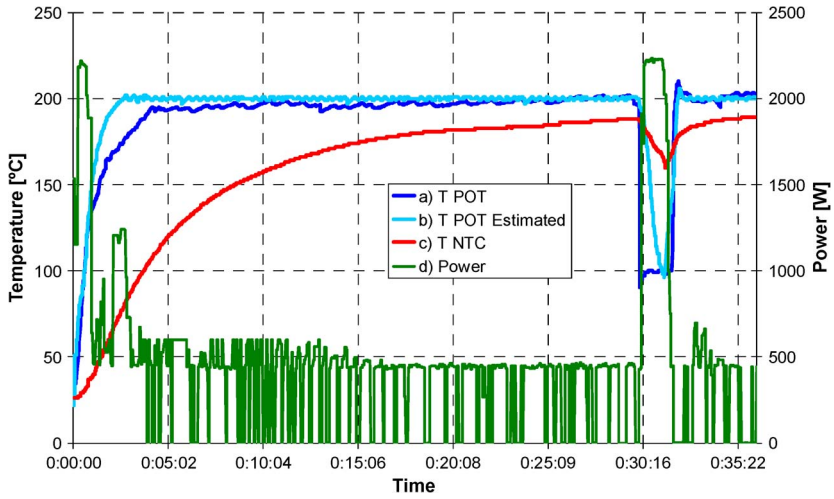

Fig. 17. Temporal course of a real test. Pan used has different thermal properties than the model chosen. (a) Represents the real pan temperature. (b) Represents the estimated pan temperature. (c) Represents the temperature measured by the NTC thermistor. (d) Represents the power supplied by the inductor.

reaches the set point for the first time but also when the water is added (about the 30 min).

C. Multiple Model Observer

In Fig. 16, we use again a real pan with the same thermal and magnetic properties than the reference model. One of the models of the multiple model observer has the same parameters than the real pot, and it is denoted by M_{R}. As expected, the control scheme selects the model M_{R} as the best one.

Results obtained with the reference pot are, in that case, quite similar to the obtained with the adaptive observer. Multiple model observers bring the pan temperature to the set point in less than 2 min and without overshoot and with $\pm 2\ ^{\circ}\mathrm{C}$ of steady state offset.

In Fig. 17, we show the results of a real pan with different thermal and magnetic properties than every model available on the multiple model observer. As the model chosen has not the same thermal behavior, the pot temperature estimation and the real pot temperature do not match perfectly. Anyway, as is shown above, the plant has a better transient behavior than the same plant controlled by the adaptive observer.

In this case, the multiple model observer brings the pan temperature to the set point in less than 4 min, without overshoot and with $\pm 8\ ^{\circ}\mathrm{C}$ of steady state offset.

V. Conclusion

In this paper, a new pan temperature control for induction hobs is described. It is based on the knowledge of the induction heating process which allows one to represent the heat transmission from the induction coil to the pan with a state-space model.

As the pan temperature is not accessible during household conditions, it has to be estimated using the measurements of the NTC thermistor placed below the ceramic glass. As induction heating is highly depending on the pan properties, two different adaptive strategies, to guarantee an accurate estimation of the temperature of any pan, are proposed. Both are compared with a conventional PID controller without an adaptive observer. The poor performance obtained in that case highlight the advantages of using an adaptive observer strategy.

Both proposed control schemes allow one to control the cooking temperature, but the control scheme using multiple models has a better transient behavior than using conventional adaptive observer when pot used has different thermal properties than expected. Therefore, the multiple model observer is chosen for the final control scheme.

The complete control scheme is cheap, simple, safe, robust, and very user friendly. It is applied in present consumer induction hobs for automatic cooking.

References

[1] S. Koide and S. Hiejima, "Temperature controlled induction heating and cooking apparatus," U.S. Patent 4 617 441, Oct. 14, 1986.
[2] U. Has, J. Schieferdecker, and D. Wassilew, "Infrared sensor to control temperature of pans on consumer hobs," in *Proc. Int. Congr. OPTO*, Erfurt, Germany, May 1998, pp. 247–250.
[3] U. Has, J. Schieferdecker, and D. Wassilew, "Temperature control for food in pots on cooking hobs," *IEEE Trans. Ind. Electron.*, vol. 46, no. 5, pp. 1030–1034, Oct. 1999.
[4] R. L. Carroll and D. P. Lindorff, "An adaptive observer for single input single output linear systems," *IEEE Trans. Autom. Control*, vol. AC-18, no. 5, pp. 428–435, Oct. 1973.
[5] G. Kreisselmeir, "Adaptive observers with exponential rate of convergence," *IEEE Trans. Autom. Control*, vol. AC-22, no. 1, pp. 2–8, Feb. 1977.
[6] G. Lüders and S. Narendra, "An adaptive observer and identifier for a linear system," *IEEE Trans. Autom. Control*, vol. AC-18, no. 5, pp. 496–499, Oct. 1973.
[7] K. S. Narendra and J. Balakrishnan, "Improving transient response of adaptive control systems using multiple models and switching," *IEEE Trans. Autom. Control*, vol. 39, no. 3, pp. 1861–1866, Sep. 1994.
[8] K. S. Narendra and J. Balakrishnan, "Adaptive control using multiple models," *IEEE Trans. Autom. Control*, vol. 42, no. 2, pp. 171–187, Feb. 1997.
[9] S. Llorente, F. Monterde, J. M. Burdio, and J. Acero, "A comparative study of resonant inverter topologies used in induction cooking," in *Proc. IEEE APEC*, pp. 1168–1174.
[10] J. M. Burdío, F. Monterde, J. R. García, L. A. Barragán, and A. Martínez, "A two-output series-resonant inverter for induction-heating cooking appliances," *IEEE Trans. Power Electron.*, vol. 20, no. 4, pp. 815–822, Jul. 2005.
[11] J. Acero, J. I. Artigas, J. M. Burdío, L. A. Barragán, and S. Llorente, "Power measuring in two-output resonant inverters for induction cooking appliances," in *Proc. IEEE PESC*, 2002, pp. 1161–1166.

Authorized licensed use limited to: Universidad de Zaragoza. Downloaded on May 21, 2009 at 10:45 from IEEE Xplore. Restrictions apply.

[12] J. Acero, D. Navarro, L. A. Barragán, I. Garde, J. I. Artigas, and J. M. Burdío, "FPGA-based power measuring for induction heating appliances using sigma-delta A/D conversion," *IEEE Trans. Ind. Electron.*, vol. 54, no. 4, pp. 1843–1852, Aug. 2007.

[13] J. Acero, J. M. Burdío, L. A. Barragán, D. Navarro, R. Alonso, J. R. Garcia, F. Monterde, P. Hernandez, S. Llorente, and I. Garde, "The domestic induction heating appliance: An overview of recent research," in *Proc. IEEE APEC*, 2008, pp. 651–657.

David Paesa received the M.Sc. degree from the University of Zaragoza, Zaragoza, Spain.

Since 2006, he has been with the Department of Computer Science and Systems and with the Research and Development Department for Induction, BSH Bosch Siemens Home Appliances, Zaragoza. He has been working on temperature control applications and energy-saving appliances. His interests include microprocessor-based control, robust and adaptive control, adaptive and multimodel observers, as well as energy-saving technologies.

Sergio Llorente received the M.Sc. degree from the University of Zaragoza, Zaragoza, Spain.

Since 2001, he has been with BSH Bosch Siemens Home Appliances, Zaragoza, where he has been the Leader of Induction Electronics and Automatic Cooking, in the Research and Development Department for Induction Hobs, since 2004. He has also been an Assistant Professor with the University of Zaragoza since 2004. His interests include power electronics, simulation and control algorithms for power electronics, and temperature control.

Carlos Sagüés received the M.Sc. and Ph.D. degrees from the University of Zaragoza, Zaragoza, Spain.

During the course of his Ph.D. studies, he was working on force and distance sensors for robots. Since 1994, he has been with the Department of Computer Science and Systems Engineering—Aragon Institute for Engineering Research, University of Zaragoza, as an Associate Professor, where he has also been the Head Teacher. He lectures on control engineering and robotics for B.Sc. students and he lectures on control engineering and 3-D computer vision for M.Sc. students. His current research interests include visual control and control engineering, and he has authored several conference and journal papers related to these topics.

Óscar Aldana received the M.Sc. degree from the University of Zaragoza, Zaragoza, Spain.

Since 2005, he has been with the Induction Cookers Software Department, BSH Bosch Siemens Home Appliances, Zaragoza, where he has been working on multisensor integration, wireless communication, temperature control, and energy saving for home appliances. His interests include microelectronics, simulation and control algorithms, wireless and communication systems, as well as real-time embedded developments.

Authorized licensed use limited to: Universidad de Zaragoza. Downloaded on May 21, 2009 at 10:45 from IEEE Xplore. Restrictions apply.